**DATA REPOSITORY (D.R.) 2013053 SUPPLEMENTARY INFORMATION**

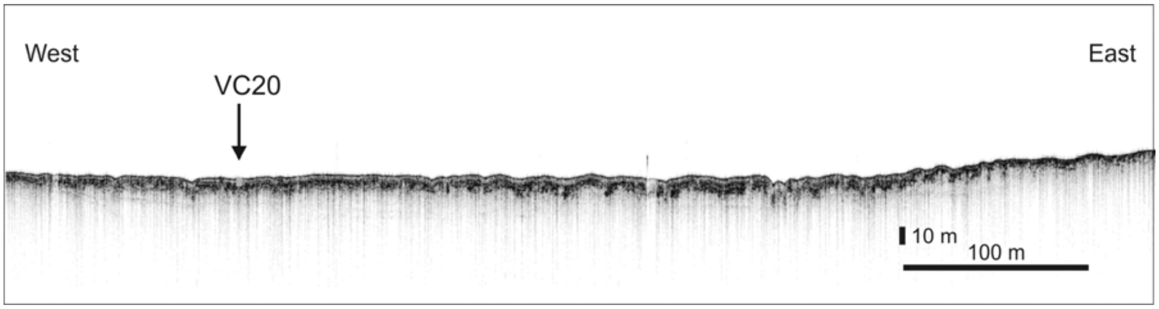


*D.R. Figure 1. TOPAS sub-bottom profiler record from the mid-shelf section of Disko Trough in about 400 m water depth showing the acoustic stratigraphy at the core site of VC20. The acoustically transparent sediment drape in the upper part of the record corresponds to a suite of fine-grained glacimarine muds in the upper 3.5 m of the core.*

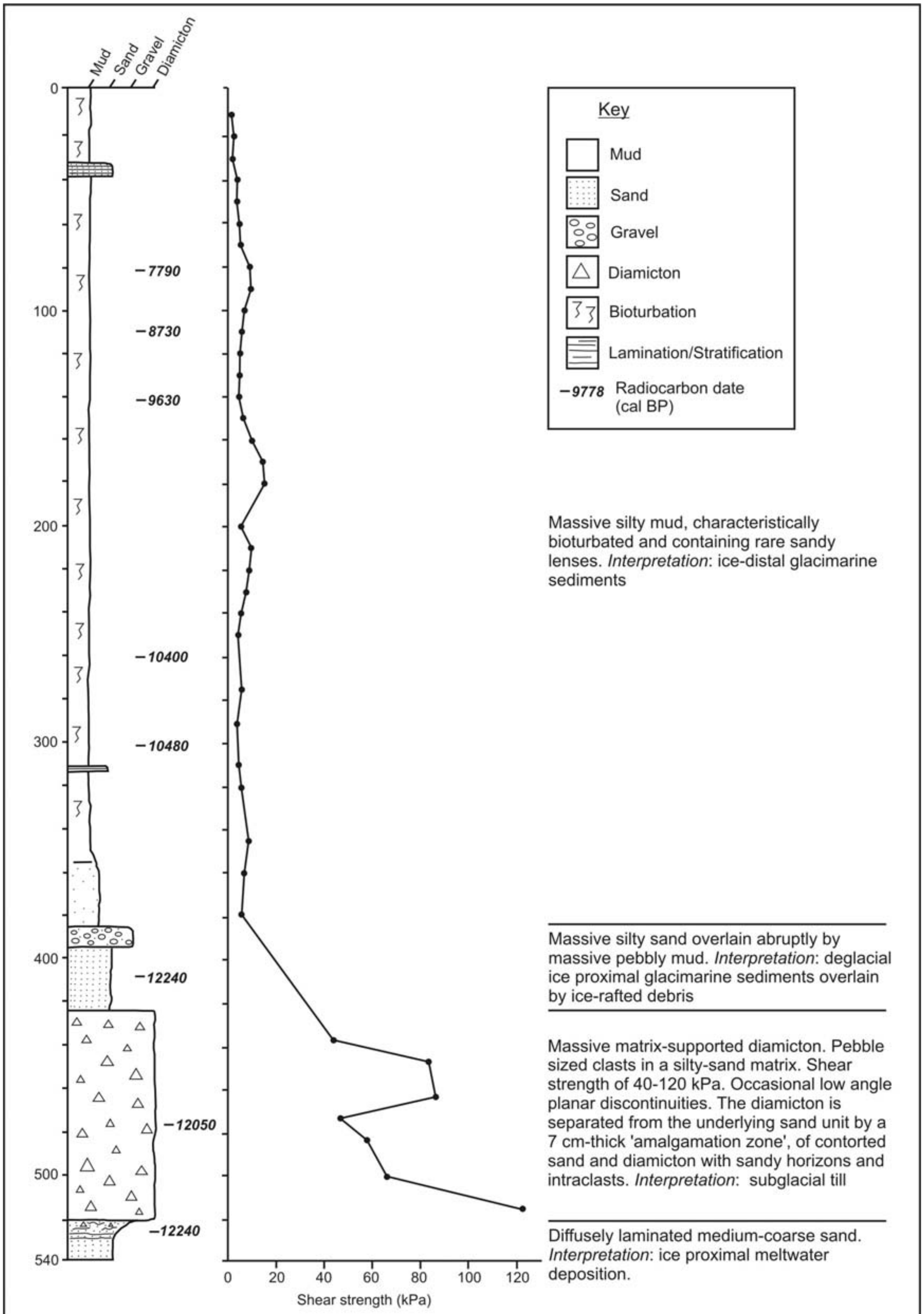


*D.R. Fig. 2. Sedimentary log, shear strength plot and facies interpretation of VC20, outer Disko Trough. Calibrated radiocarbon dates in italics. See also D.R. Table 2.*

## Microscopic analysis of the JR175 VC20 diamicton

The diamicton in VC20 is massive and predominantly silty, with dispersed, fine to medium, subrounded to subangular pebbles. Clasts are volcanic and metamorphic, with smaller grains predominantly of quartz composition. Hornblende is relatively common, which may point to a volcanic derivation. Microfossils are common throughout. Shell fragments, some up to several mm long, are particularly common between 488-495 cm. There are also examples of degraded marine diatoms (and fragments), possibly *Hemidiscus* or *Coscinodiscus*[SR1], and *intact* multi-chambered, planktonic foraminifera.

Visually, the plasma (matrix) material has a high fine to medium silt, and a low clay content. While in the 488-495 and 447-451 cm the plasma density is fairly uniform, between 450-456 cm it is more heterogeneous in character with poorly defined, fine-textured zones (clay to fine silt) delineated by 'tracks' or zones which are relatively silt-rich (or poor in clay). This suggests a degree of sorting (water percolation/escape) and associated (re-)mobilization or winnowing of fines. In this interval pebble density is relatively high with a significant area taken up by irregularly shaped voids.

Between 490-495 cm, there are some poorly defined, parallel, subhorizontal silt-rich zones (up to a few mm thick) in which grains tend to be relatively angular. These observations lead to the tentative inference that localized grain fracturing may have played a role, although no examples of *in situ* fractured grains were identified[SR2]. Possibly associated with these zones are a number of subhorizontal planar fractures, some of which are cm long. Also seemingly associated are short 'streaks' (mm long) of plasma with an increased density that line up with some of the fractures.

The subhorizontal signal in this part of the core is also reflected in the occurrence of 'lineaments', i.e. arrangements of three or more grains with long axes parallel to their subhorizontal alignment[SR3]. At high magnifications and in cross-polarized light, very thin and weakly developed short/discontinuous unistrial plasmic fabric can be identified along some of the constituent grains of these lineaments.

Again between 490-495 cm, there are common examples of circular patterns (some of which are turbates – finer grains aligned around coarser core grain[SR3, SR4]. Largest features are in the order of 2-3 mm across, but most are much smaller (tens to hundreds of microns across). Between 447-456 cm, circular grain arrangements are more abundant (and dispersed throughout), again ranging in size from a few tens of microns to mm across.

Around 452 cm, on the RHS, some (dis)continuous curvilinear fine fractures outline a cm-scale rounded, elongated 'aggregate'. It displays the same overall characteristics as the surrounding sediment, although it has slightly denser plasma. Curiously, this rounded aggregate shows a strong preferred microfabric signal, more or less parallel to the long axis of the aggregate (and not different from the surrounding sediment; see below). There is also one example of a rounded intraclast at 448-449 cm, c. 5 mm in diameter, consisting of predominantly mud with indistinct boundaries to the surrounding matrix.

Following a procedure described by Phillips et al.[SR5], long axis orientations of particles coarser than medium silt were digitized in both core intervals. Based on preferred signals emerging from rose plots that were generated for sub-areas of the thin sections, azimuth classes were defined, which were subsequently used to identify and map clusters of grains with similar orientations.

The mapping exercise produced the following microfabric signals (reflected in both core intervals):

1. 000º-010º (and 180º-190º)
2. 040º-050º (and 220º-230º)
3. 130º-150º (and 310º-330º)
4. 100º-125º (and 280º-305º)
5. 090º-100º (and 270º-280º)

Signal 1 occurs exclusively along the margins of the core intervals. In the upper core interval it is also closely related to irregular voids parallel to the sides of the core, which strongly suggests that this signal is an artefact resulting from drag in the vibro-coring process. Signals 2 and (the shallower range of) signal 3 constitute a symmetrical conjugate set of directions (i.e. 45º-315º), and occur patchily in both core intervals. They are attributed to pure shear, again likely related to the coring process.

More interesting are the steeper range of signal 3 (140º-150º (and 320º-330º) and signal 4 (continuing into sub-horizontal signal 5). Signals 4 and 5 are superimposed on signal 3 and it is inferred that both may be related to the same process of simple shear. Whereas the steeper range of signal 3 is thought to represent an early stage of deformation (it is particularly pervasive between 477-456 cm), signal 4 is the most prominent signal in both samples, and is thought to be the reflection of the final stages of strain. Signal 5 is patchy, but compatible with the subhorizontal features identified in 490-495 cm (linear fractures, grain lineaments and unistrial plasmic fabrics).

Highlighted in D.R. Figs. 3A (447-456 cm) and 3C (488-495 cm) are the visually established zones with clusters of grains that are preferentially oriented in the Signal 4 range. The pattern that emerges is one of discrete, parallel zones that may be discontinuous, but nevertheless cover the full core width. These zones are interspersed and cross-cut by the conjugate signals 2 and 3. This would reinforce the idea that the latter are coring artefacts. Signals 4 and 5 occur throughout 488-495 cm, whereas in 447-451 cm they are concentrated in the upper core interval. In fact, the lower part of this interval (451-456 cm) shows no extensive zones of any of the preferred orientations identified.

D.R. Figures 3B (447-456 cm) and 3D (488-495 cm) are an attempt to statistically corroborate the results of 3A and 3C. Again employing the mask highlighting Signal 4, the dots represent computed probability clusters of grains showing this range of orientations (relative to a Bernoulli discrete distribution). For both core intervals (Figs. 3B and 3D) the distribution of dots are largely compatible with the visually mapped zones (Figs. 3A and 3C, respectively). The shading and contouring represent the spatial relative strength of the clustered signals. Note that the colour schemes are mirrored and that the values given for the two core intervals in the respective keys cannot be cross-compared.

*Interpretation*

The presence of marine fauna in both core intervals suggests that the diamicton contains recycled (glaci-) marine sediment. Both core intervals exhibit features that are common for subglacially sheared materials (subglacial traction tills). The parallel zones of preferred microfabrics, the subhorizontal fractures and associated features such as plasma streaks, zones of fractured grains, turbates, soft sediment intraclasts, and lineaments are interpreted as an expression of strain in response to imposed simple shear stresses. In the upper core interval, strain was apparently concentrated in the upper part. In the lower part of the upper core interval, the strain signature was either lost due to subsequent (artificial) disturbance, or simple shear, as generated by overriding ice, was concentrated at discrete levels within the till only (strain partitioning).

## Supplementary References (SR)


[SR1] Harwood, D.M., 1986. Do Diatoms beneath the Greenland Ice Sheet Indicate Interglacials Warmer than Present? Arctic 39(4), 304-308

[SR2] Hiemstra, J.F. and van der Meer, J.J.M. 1997. Pore-water controlled grain fracturing as indicator for subglacial shearing in tills. Journal of Glaciology 43 (145), 446-454.

[SR3] Hiemstra, J.F. and Rijsdijk, K.F. 2003. Observing artificially induced strain: implications for subglacial deformation. Journal of Quaternary Science 18(5), 373-383.

[SR4] van der Meer, J.J.M. 1993. Microscopic evidence of subglacial deformation. Quaternary Science Reviews 12, 553–587.

[SR5] Phillips, E.R., van der Meer, J.J.M. and Ferguson, A. in press. A new 'microstructural mapping' methodology for the identification, analysis and interpretation of polyphase deformation within subglacial sediments. Quaternary Science Reviews.

[SR6] McNeely, R., Dyke, A.S. and Southon, J.R., 2006, Canadian marine reservoir ages, preliminary data assessment: Geological Survey Canada Open File, v. 5049, pp. 3.

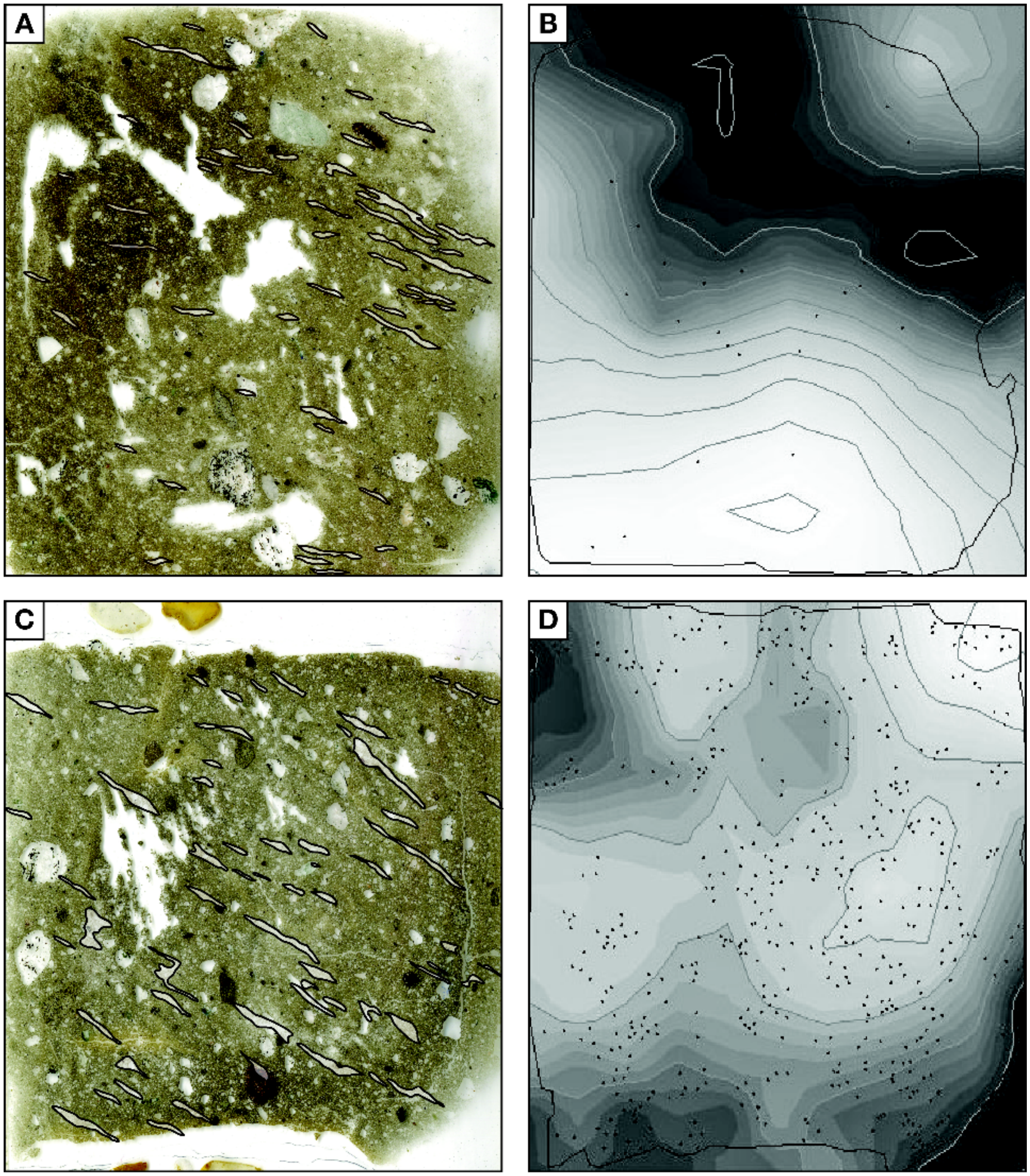


*D.R. Figure 3. Microfabric analysis of the VC20 diamicton. Panels A and C represent core interval 447-456 cm, and panels B and D represent core interval 448-495 cm. Panels A and C are scans of the thin-sectioned samples; highlighted is the distribution of zones with microfabrics in the range 100º-125º (signal 4). Panels B and D show maps generated in Rockworks15 (Rockware®) indicating clusters of preferred orientations (dots) and the strength of the signal (shading). For further explanation see text.*

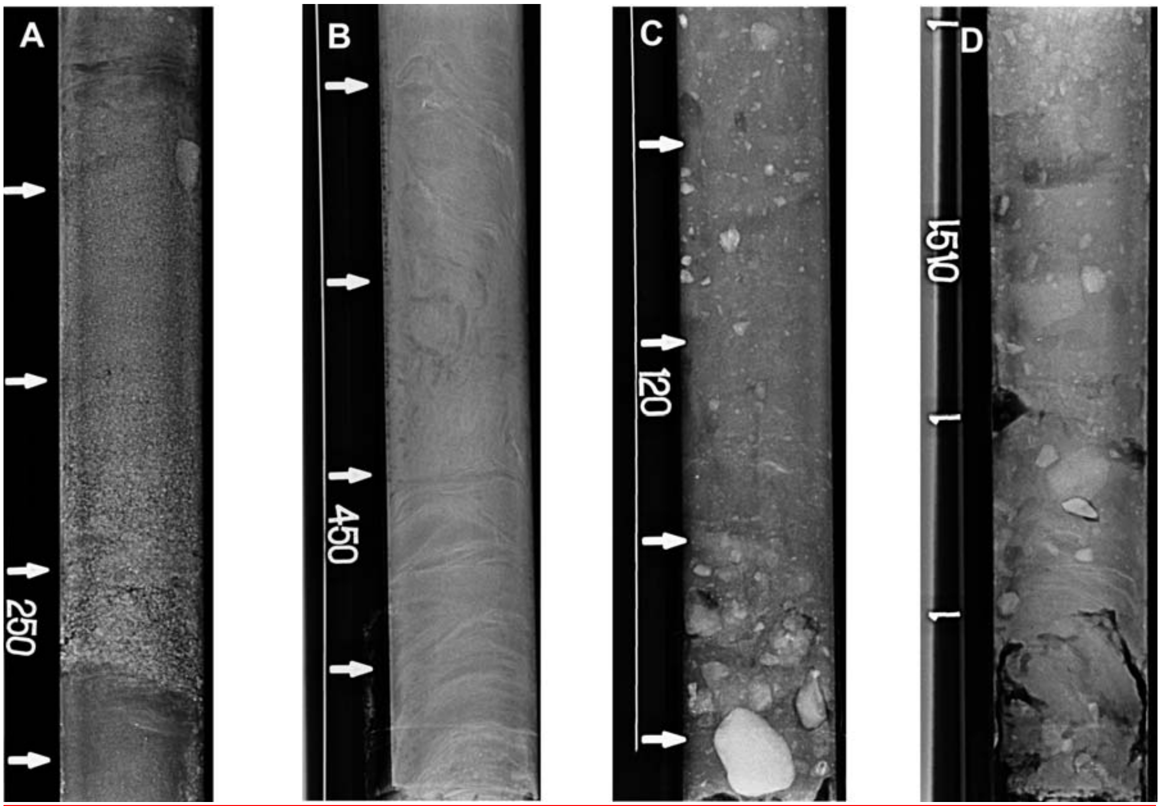


*D.R. Figure 4. X-radiographs of lithofacies from sediment cores from the Disko Fan, outer Disko Trough and outermost Uummannaq Trough. (A) Disko Fan, core VC34, 224-261 cm depth. Normally graded sand unit interpreted as a turbidite (Bouma Division A). Note sharp lower contact at 255 cm depth and isolated clast interpreted as IRD at 229 cm depth. (B) Disko Fan, core VC35, 427-465 cm depth. Highly contorted laminated mud from 427-450 cm depth overlying undeformed to lightly contorted laminated mud. These sediments are interpreted as a product of downslope sediment delivery by turbidity currents. The highly contorted nature of the sediments above 427 cm depth is thought to represent post-depositional slumping of the turbidites. Below 450 cm depth the downward turned laminae are regarded as a product of deformation during the coring process. (C). Uummannaq Trough, outermost shelf, core VC45, 105-142 cm depth. The lower part of the core below 130 cm depth comprises a stiff massive diamicton interpreted as a subglacial till. This is overlain by a thin (4-5 cm thick) zone of diffusely laminated mud from which a sample of benthic formaminfera (Cassidulina neoteretis) dated 14,880 yr BP, and is overlain in turn by massive mud with scattered clasts, mostly of small pebble size. The diffusely laminated mud and overlying massive mud with IRD is interpreted as recording increasingly ice-distal conditions during deglaciation. (D) Disko Trough, outer shelf, core VC20, 500-539 cm depth. The lowermost unit from 539-520 cm comprises diffusely laminated sand; this is overlain by stiff (40-120 kPa – see article Figure 3) massive, matrix-supported diamicton with occasional low-angle planar discontinuities. The sand is separated from the diamicton by a 7 cm-thick 'mixed zone' of contorted sand and diamicton. The diamicton is interpreted as a subglacial till and the underlying sand as a product of meltwater sedimentation.*

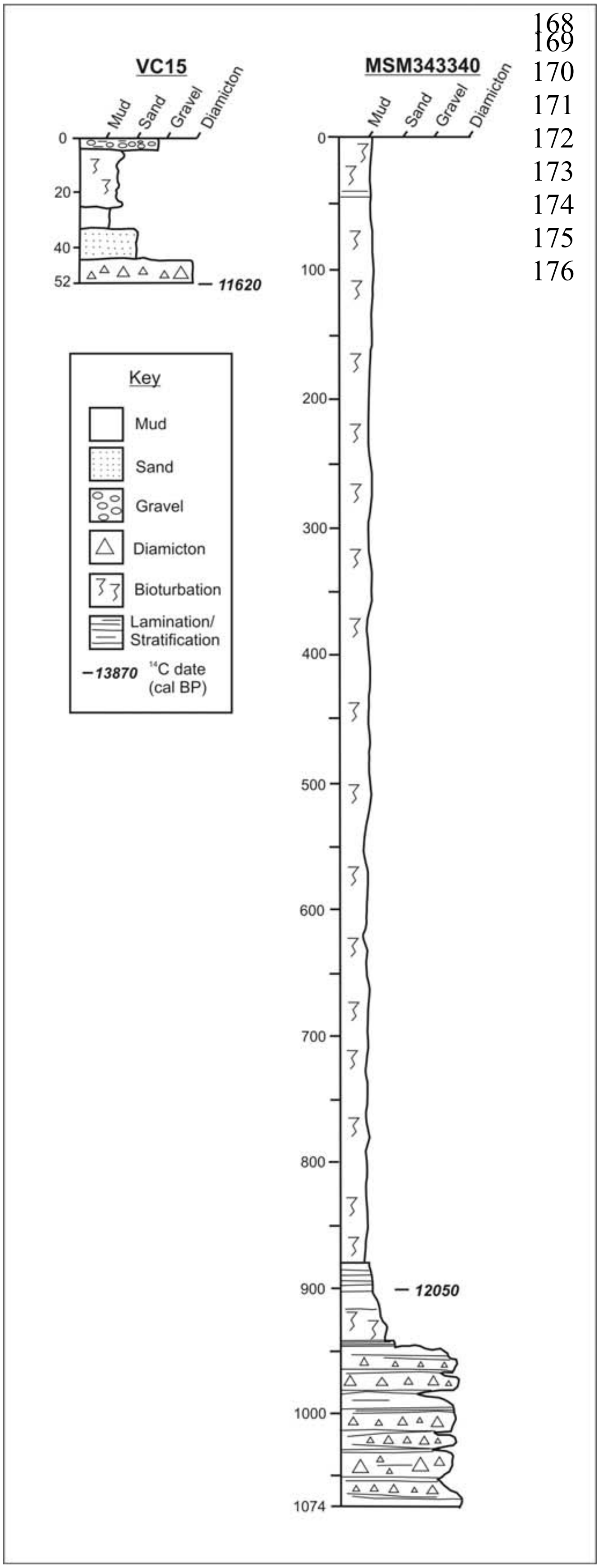


*D.R. Fig. 5. Sedimentary logs of cores from outermost Disko Trough (VC15) and mid-shelf Disko Trough (MSM343340). See Figure 1 for locations of cores and Data Repository Table 2 for details on radiocarbon dates*.

D.R. Table 1. Site information on sediment cores from Disko and Umanak troughs and the Disko Fan

| **Core number** | **Grid reference** | **Location** | **Water depth** | **Core length (cm)** | **Geomorphological setting** |
|---|---|---|---|---|---|
| VC15 | 67º 54.53’N 058º 43.91’W | Outermost Disko shelf in front of ‘moraine’ | 347 m | 55 | |
| VC20 | 68º 12.06’N 057º 45.38’W | Disko Trough, outer shelf. | 424 m | 539 | |
| MSM343340 | 68º36’55’’N 055º19’59’’W | Disko Trough, mid-shelf | 461 m | 1074 | |
| VC34 | 67º 33.36’N 059º 53.03’W | Disko Fan. | 1476 m | 345 | Disko fan. Channel floor. |
| VC35 | 67º 42.03’N 059º 20.54’W | Disko Fan. | 1267 m | 536 | Disko Fan. Levee. |
| VC45 | 70º 33.99’N 060º 18.45’W | Umanak Trough | 648 m | 141 | Crest of shelf-edge moraine |

D.R. Table 2. Radiocarbon dates from Disko and Umanak troughs and the Disko Fan, west Greenland

| **Core** | **Lab code** | **Sample depth (cm)** | **Material** | **$^{14}C$ age** | **cal BP range**<br>**[a] 1 sigma**<br>**[b] 2 sigma** | **Calibrated age** |
|---|---|---|---|---|---|---|
| VC20 | BETA-265217 | 524-525 | Nuculana pernula (single valve) | 10910+60 | 12084-12335 [a]<br>11952-12522 [b] | 12240 |
| VC20 | BETA-265216 | 477.5-478 | Shell fragment | 10840+60 | 11941-12194 [a]<br>11757-12346 [b] | 12050 |
| VC20 | AA-91731 | 408 | Shell fragment | 10914+59 | 12091-12340 [a]<br>11958-12523 [b] | 12240 |
| VC20 | BETA-265215 | 301-303 | Nuculana pernula (paired valves) | 9780+50 | 10457-10567 [a]<br>10358-10607 [b] | 10480 |
| VC20 | BETA-265214 | 261-262 | Nuculana pernula (paired valves) | 9700+50 | 10358-10507 [a]<br>10263-10540 [b] | 10400 |
| VC20 | AA-90389 | 140-141 | Seaweed | 9030+200 | 9356-9887 [a]<br>9116-10149 [b] | 9630 |
| VC20 | AA-90388 | 110-111 | Seaweed | 8300+180 | 8462-8920 [a]<br>8281-9173 [b] | 8730 |
| VC20 | AA-90387 | 80-81 | Seaweed | 7464+66 | 7702-7860 [a]<br>7646-7931 [b] | 7790 |
| VC15 | BETA-265212 | Core catcher | Shell fragment | 10620+60 | 11391-11740 [a]<br>11323-11915 [b] | 11620 |
| VC34 | BETA-265221 | 316 | Shell fragment | 23310+160 | 27016-27871 [a]<br>26866-28006 [b] | 27440 |
| VC34 | BETA-265220 | 253-254 | Shell fragment (Nuculana pernula | 21770+100 | 25103-25531 [a]<br>24983-25777 [b] | 25380 |
| VC34 | BETA-272270 | 183 | Shell fragment | 12740+70 | 13927-14153 [a]<br>13808-14518 | 14160 |
| VC34 | BETA-272269 | 160-161 | Shell fragment | 12550+70 | 13774-13944 [a]<br>13685-14047 [b] | 13870 |
| VC34 | BETA-272268 | 130-132 | Shell fragment | 12050+60 | 13289-13416 [a]<br>13199-13506 [b] | 13350 |
| VC34 | BETA-272267 | 99 | Shell fragment | 12490+70 | 13719-13898 [a]<br>13598-14005 [b] | 13800 |
| VC35 | BETA-272271 | 174.5-176.5 | Shell fragment | 10940+60 | 12107-12362 [a]<br>12005-12544 [b] | 12270 |
| VC35 | BETA-265222 | 482-483 | Nuculana pernula (single valve) | 15380+70 | 17896-18465 [a]<br>17722-18514 [b] | 18120 |
| MSM343340 | POZ-30991 | 901-902.5 | Portlandia arctica (paired valves) | 10840+60 | 11941-12194 [a]<br>11757-12346 [b] | 12050 |
| VC45 | AA-89913 | 125-127 | Mixed benthic foraminifers | 13211+92 | 14677-15177 [a]<br>14243-15519 [b] | 14880 |

All calibrations were carried out using the Marine 09.14c dataset and Calib 6.0. A $\Delta R$ of 140 years ± 25 was applied to the West Greenland dates based on http://calib.qub.ac.uk/marine/ and McNeely et al. 2006[SR6].
Calibrated ages listed in final column are the mean of the 2δ calibrated age range and have been rounded to the nearest 10 years.
‘$^{14}C$ age’ is the measured radiocarbon age corrected for isotopic fractionation, calculated using delta 13C.